Global Net-gain Characterization of Monolithically Integrated Waveguide Amplifiers

Jinfeng Mu, Meindert Dijkstra, Sonia García-Blanco
Integrated Optical Systems, MESA+ Institute for Nanotechnology, University of Twente,
PO Box217, 7500AE, Enschede, The Netherlands
Author e-mail address: s.m.garciablanco@utwente.nl

Abstract: Global net-gain characterization is presented for the monolithically integrated $Al_2O_3:Er^{3+}$-Si_3N_4 amplifiers by comparing the amplified signal to the output of the passive reference waveguides, showing good agreement with the conventional signal enhancement method.

1. Introduction

The rapid evolution of integrated photonics significantly requires to increase the number of integrated components per circuit for more advanced functionality. The growing number of total on-chip losses highlights the importance to realize on-chip optical amplifiers especially towards optical network improvement and cost reduction [1]. Besides the semiconductor optical amplifiers (SOAs), erbium doped waveguide amplifiers (EDWAs) attract research interests in numerous materials such as Al_2O_3 [2], TeO_2 [3] and lithium niobate [4], due to the long lifetime (0.1-10 ms) of the rare-earth ions and lower optical nonlinearity with respect to SOAs, which benefits high-bit rate amplification [5, 6], reducing both signal degradation and intermodulation. Erbium ion doped amorphous Al_2O_3 ($Al_2O_3:Er^{3+}$) shows promising features including broadband gain (~80 nm), high net gain (~20 dB) and highly tolerant and scalable fabrication process [7].

Previously, we demonstrated high-gain monolithically integrated $Al_2O_3:Er^{3+}$-Si_3N_4 waveguide amplifiers [8] using a double-layer photonic platform [9]. Similar as the works of [3-8], the net gain of the amplifiers is indirectly measured using the conventional the signal enhancement (SE) method, requiring precise characterization of the absorption and propagation loss of the gain waveguide and other on-chip component losses. In this paper, we present a global net-gain characterization to directly obtain the net-gain from the measured output signal powers from the amplifier and a passive reference waveguide.

2. Characterization Design and Results

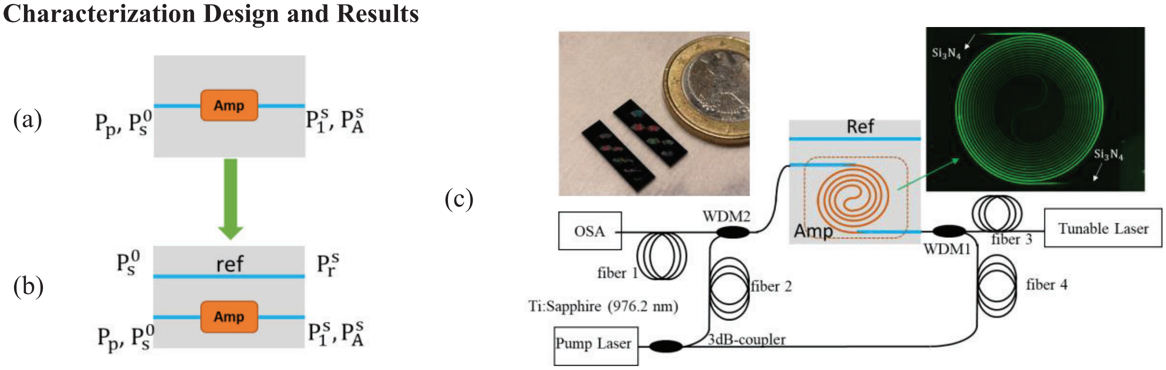

Fig. 1. Gain characterization schematics for the waveguide amplifier chips (a) without and (b) with passive reference waveguide. (c) Experiment setup used for gain characterization with bidirectional pumping scheme.

The conventional signal enhancement (SE) method with the power parameters is shown in Fig. 1(a). In the pump-off case, the output signal (P_1^s) is equal to the input signal (P_s^0) subtracting the fiber-to-chip coupling loss, the absorption loss ($\alpha_{a,s}$), the propagation loss (α_0) and the $Al_2O_3:Er^{3+}$-Si_3N_4 coupler loss (α_c). In the pump-on case, the net gain is equal to the ratio of the output signal (P_A^s) to the input signal (P_s^0). In the SE method, the measured powers are P_1^s and P_A^s, from which it can be derived the expression for the net gain, g_{SE} as expressed by eq. (1).

$$g_{SE} = 10\log_{10}(P_A^s)/(P_1^s) - \alpha_{a,s} - \alpha_0 - 2\alpha_c \tag{1}$$

$$g_{global} = 10\log_{10}(P_A^s)/(P_r^s) \tag{2}$$

Benefiting from the active-passive integration based on our monolithic photonic platform [9], the global net gain can be directly characterized by comparing the amplified signal of the amplifier in the pump-on case (P_A^s) to the signal of the reference waveguide that is passive (P_r^s) using eq. (2), which includes all on-chip losses. Waveguide facets on the same chip after dicing are assumed to be identical, resulting in same fiber-to-chip coupling efficiencies between the reference waveguide and the integrated amplifier. Therefore, the integrated amplifier can be considered as a building block. The measured global net-gain immediately indicates the building block performance, i.e., the amplification capability.

Comparing to the conventional method, the global net-gain characterization does not require to measure the absorption and propagation losses, and on-chip component losses like the Al_2O_3:Er^{3+}-Si_3N_4 coupler individually for each amplifier chip. Secondly, it accounts all on-chip losses and yields a more robust result to the waveguide imperfections. Thirdly, the unabsorbed signal power from the reference waveguide and the amplified power are relatively large, making the detection of these signals easier especially for amplifiers with high absorption loss or long propagation distances, where the output signal power in pump-off case, P_1^s, can be very weak and requires highly sensitive detectors and other technologies to enhance the signal-to-noise ratio (SNR).

Fig. 1(c) depicts the experiment setups employed in his work for the global net-gain characterization. The pump light at 976.2 nm is provided by a Ti:Sapphire laser. The signal light at 1532 nm is from a tunable laser (Agilent 8164B). TE polarization is used for the signal. The output signal in the pump-on and pump-off cases are measured by an optical spectrum analyzer (OSA). The pump is split by a 3 dB coupler and launched into both sides of the chip. This bidirectional pumping scheme is advantageous to invert the integrated Al_2O_3:Er^{3+} spiral more uniformly throughout its length, which avoids the depletion of the pump by a strong amplified signal power followed by strong absorption of the amplified signal for the increasing length. The pump and signal are externally combined or split using polarization maintaining (PM) wavelength division multiplexers (980/1550 WMD). At the output, the pump and signal are collected and connected to the OSA where the residual pump is further removed.

In pump-off case, the absorption plus propagation losses (dB/cm) in the spectral window of 1460–1638 nm under different incident powers ranging from 0 dBm to -30 dBm (output powers from the laser) are characterized by comparing the output signal power P_1^s of the amplifier waveguide to that of the reference output P_r^s. A coupler loss of 0.64±0.2 dB is measured at 1306 nm wavelength, which lies outside the ground state absorption band of Er^{3+} ions. With the measured coupler loss, the absorption plus propagation losses can be extracted from the insertion losses, which is about 3 dB/cm at 1532 nm. Additionally, the spectra converge for incident powers below -20 dBm, which corresponds to the start of the small signal regime. Fig. 2(b) shows the transmission spectra of the reference Si_3N_4 waveguide in pump-off and pump-on cases. Transmission values (plotted by dots) are extracted after eliminating the ASE from the spectra using similar approach as in [8]. The incident power at 1532 nm is -30 dBm. The global net-gain of 9 dB can be directly obtained by subtracting the reference output from the amplified signal power in dBm. Furthermore, the signal enhancement of ~31.2 dB can also be observed from the measured signal spectra in pump-on and pump-off cases. According to eq. (1), the net-gain of 8.3 dB can be calculated. The global net-gain has good agreement with the net-gain obtained from signal enhancement but with much simpler and direct realization.

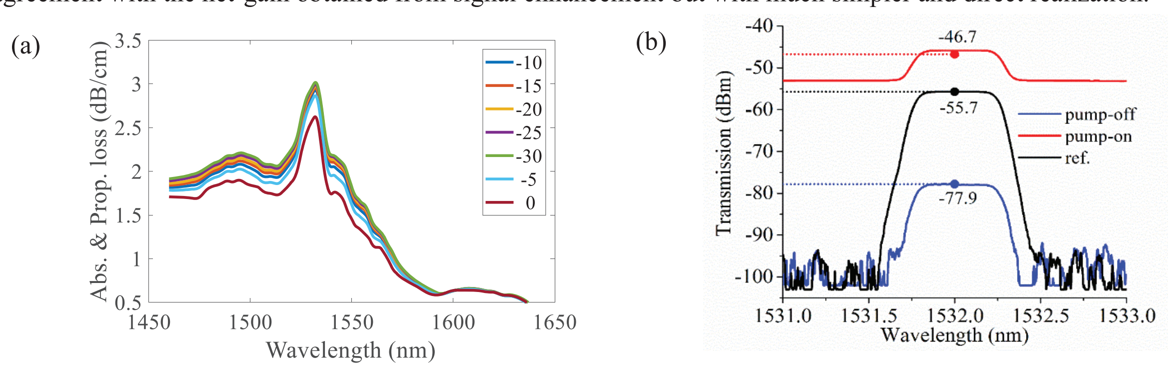

Fig. 2. (a) Absorption plus propagation loss (α_{ap}) per unit length of the integrated amplifier at different incident signal powers in the spectral window of 1460–1638 nm. (b) Measured spectra from the OSA for the reference Si_3N_4 waveguide, and the integrated amplifier in pump-on and pump-off cases at 1532 nm. The incident signal power -30 dBm. The OSA resolution is adjusted to 0.5 nm. The Al_2O_3:Er^{3+} length is 7.2 cm.

3. References

[1] C. Vagionas et al., J. Lightwave Technol., 1-1 (2021). https://doi.org/10.1109/JLT.2021.3131130
[2] W. A. P. M. Hendriks et al., Advances in Physics: X 6, 1833753 (2021). https://doi.org/10.1080/23746149.2020.1833753
[3] H. C. Frankis et al., Photon. Res. 8, 127-134 (2020). https://doi.org/10.1364/PRJ.8.000127
[4] J. Zhou et al., Laser Photon. Rev. 15, 2100030 (2021). https://doi.org/10.1002/lpor.202100030
[5] T. Chrysostomidis et al., IEEE Photon. Technol. Lett. 33, 1177-1180 (2021). https://doi.org/10.1109/LPT.2021.3111894
[6] T. Chrysostomidis et al., J. Lightwave Technol., 1-1 (2021). https://doi.org/10.1109/JLT.2021.3121467
[7] J. D. B. Bradley et al., J. Opt. Soc. Am. B 27, 187-196 (2010). https://doi.org/10.1364/josab.27.000187
[8] J. Mu et al., Photon. Res. 8, 1634-1641 (2020). https://doi.org/10.1364/PRJ.401055
[9] J. Mu et al., IEEE J. Sel. Top. Quantum Electron. 25, 1-11 (2019). https://doi.org/10.1109/JSTQE.2019.2908559